Tunneling and anticrossing of edge magnetoplasmons in a quantum-dot superlattice

Danhong Huang and Godfrey Gumbs
Department of Physics, Massachusetts Institute of Technology, Cambridge, Massachusetts 02139
(Received 21 December 1990)

We calculate edge magnetoplasmons for a superlattice of quantum dots where a uniform magnetic field is applied along the superlattice direction. The confinement is assumed parabolic. We find (a) anticrossing of the edge magnetoplasmon modes and (b) splitting of the tunneling magnetoplasmon branch. Similarities with experimental data for a quantum-dot array within a plane are discussed.

During the past few years, both dielectric response and transport properties of mesoscopic systems have been the focus of considerable attention for theorists as well as experimentalists. In many experiments,[1,2] some aspects of the data are hard to explain in terms of the single-particle picture or by considering the motion of the center of mass[3-5] due to the fact that electrons are strongly correlated when the region in which they are confined and the separation between quantum dots are small. Recently, Demel *et al.*[1] reported the observation of anticrossing behavior for the edge magnetoplasmons in a quantum-dot array within a two-dimensional (2D) plane. To explain their data, they used a classical disk magnetoplasmon model and obtained good agreement between their theory and experiment. This model does not, however, reproduce the anticrossing feature for the edge magnetoplasmon branches since this is due to many-body effects.[6]

The purpose of this paper is to present a detailed analysis of a quantum-dot superlattice chain whose spectrum displays features similar to those in Ref. 1, although the arrangements of the quantum dots in the two cases are geometrically different. The reason for this is that there are several aspects in common between the two systems. One is that the nonlocal many-body effects (intradot Coulomb interaction) become important as the single-particle confinement becomes stronger or the number of electrons within each quantum dot becomes larger. Another is that the interdot Coulomb interaction distorts the single-particle harmonic confining potential so that it is no longer quadratic or symmetrical about the azimuthal axis in the case of 2D quantum-dot array. This distortion gets larger as the number of electrons within a dot is increased or when the separation between quantum dots is decreased. In our calculations, the self-consistent potential is a sum of a single-particle potential and the Hartree-Fock potential. Therefore, the original dipole-prohibited transitions ($|\Delta m|\neq 1$, m is the azimuthal quantum number) will be allowed and the oscillator strengths of those modes which were forbidden will increase with the degree of distortion and the amount of level mixing, near-resonant anticrossing, or at large magnetic fields. We believe that the highest branch of the excitation spectrum ($\omega_{2\pm}$ in the notation of Fig. 2 in Ref. 1) corresponds to the prohibited modes ($\Delta m=0,-2$).

Here, we consider a chain of quantum dots forming a superlattice along the z axis. We assume a parabolic confining potential $\frac{1}{2}m^*\Omega_0^2 r^2$ in each plane. In cylindrical coordinate, the Hamiltonian of a quantum-dot superlattice with a magnetic field B along the z axis is given by

$$\mathcal{H}=-\frac{\hbar^2}{2m^*}\left[\frac{1}{r}\frac{\partial}{\partial r}\left[r\frac{\partial}{\partial r}\right]+\frac{1}{r^2}\frac{\partial^2}{\partial\phi^2}+\frac{\partial^2}{\partial z^2}\right]+\tfrac{1}{2}m^*\Omega_0^2 r^2+V_{\rm eff}(z)-\left[\frac{ie\hbar B}{2m^*c}\right]\frac{\partial}{\partial\phi}+\frac{e^2B^2}{8m^*c^2}r^2 , \tag{1}$$

where m^* is the electron effective mass. In this notation, the superlattice electrostatic potential is

$$V_{\rm eff}(z)=\begin{cases}0, & -L_W/2+ld<z\le L_W/2+ld ,\\ V_0, & L_W/2+ld<z\le -L_W/2+(l+1)d ,\end{cases} \tag{2}$$

where $l=0,\pm1,\pm2,\ldots,\pm\infty$, L_W and L_B are the widths of the well and barrier, respectively, and $d=L_W+L_B$ is the period. The electron wave function is

$$|n,m,k_z\rangle=\frac{1}{\sqrt{2\pi}}\exp(im\phi)R_{n,m}(r)|k_z\rangle , \tag{3}$$

with

$$|k_z\rangle=\frac{1}{N^{1/2}}\sum_l\exp(ik_z ld)\xi_0(z-ld) , \tag{4}$$

$$\xi_0(z)=\frac{1}{\sqrt{\pi^{1/2}\lambda_0}}\exp\left[-\frac{z^2}{2\lambda_0^2}\right] , \tag{5}$$

$R_{n,m}(r)$ is the normalized radial wave function,[4] and the energy eigenvalues are

$$E_{n,m}(k_z)=(2n+|m|+1)\bar{\omega}+\frac{m}{2}\omega_c+\frac{W}{2}[1-\cos(k_z d)] , \tag{6}$$

with $\bar{\omega}\equiv(\Omega_0^2+\omega_c^2/4)^{1/2}$ and W is the width of the energy band, taking into account electron tunneling between ad-

jacent quantum dots along the z axis.

With the use of linear-response theory, the random-phase approximation (RPA), and the assumption that only the lowest level is partially occupied and all the other excited levels are empty, we obtain the following dispersion relation:

$$\mathrm{Det}[\delta_{ij}-\chi_{j0}(q_z,\omega)F_{ij}^{|\Delta m|}(q_z)]=0 , \tag{7}$$

where $1\le i,j\le 4$ are composite indices, e.g., $|i\rangle=|n,m\rangle$, where n is the radial quantum number. In this notation, $|1\rangle=|0,-1\rangle$, $|2\rangle=|0,-2\rangle$, $|3\rangle=|0,1\rangle$, $|4\rangle=|1,0\rangle$. The noninteracting irreducible polarizability is

$$\chi_{i0}(q_z,\omega)=\frac{1}{\pi d}[I(\omega)+I(-\omega)] , \tag{8a}$$

$$I(\omega)=\frac{2}{[(\hbar\omega-\hbar\omega_{i0})^2-b^2]^{1/2}}\arctan\left[[(\hbar\omega-\hbar\omega_{i0})^2-b^2]^{1/2}\frac{\sin(k_F d)}{(\hbar\omega-\hbar\omega_{i0})\cos(k_F d)-b\sin(q_z d/2)}\right] . \tag{8b}$$

Here, $b\equiv W\sin(q_z d/2)$. In the case of weak tunneling ($|b|\ll 1$), we recover the result in Ref. 7 by expanding Eq. (8b) to the first order of b with the use of a Taylor-series expansion.

$F_{ij}^{|\Delta m|}(q_z)$ is given by

$$F_{ij}^{|\Delta m|}(q_z)=\frac{4\pi e^2}{\epsilon_s}\sum_l \exp\left[-\frac{(q_z+2\pi l/d)^2\lambda_0^2}{2}\right]\int_0^\infty dr\, r\int_0^\infty dr' r' G_{|\Delta m|}\left[q_z+\frac{2\pi l}{d},r,r'\right]R_i(r')R_0(r')R_j(r)R_0(r) , \tag{9}$$

where the Green's function is calculated as

$$G_{|\Delta m|}(q_z,r,r')\equiv\begin{cases}K_{|\Delta m|}(|q_z|r)I_{|\Delta m|}(|q_z|r') & \text{for } r'\le r ,\\ I_{|\Delta m|}(|q_z|r)K_{|\Delta m|}(|q_z|r') & \text{for } r'\ge r .\end{cases} \tag{10}$$

$K_i(x),I_i(x)$ are the modified Bessel functions. $\epsilon_s=4\pi\epsilon_0\epsilon_r$ is the background dielectric constant and $\omega_{10}=\bar{\omega}-\omega_c/2$, $\omega_{20}=2\bar{\omega}-\omega_c$, $\omega_{30}=\bar{\omega}+\omega_c/2$, and $\omega_{40}=2\bar{\omega}$. The Fermi wave vector is $k_F=\pi n_{1D}/2$, where $n_{1D}=\pi a^2 n_{3D}$ and n_{3D} is the 3D electron density, and the renormalized magnetic length a is given by $a^{-4}=l_0^{-4}+l_H^{-4}$, where $l_0^2\equiv\hbar/2m^*\Omega_0$ and $l_H^2\equiv\hbar c/eB$.

A straightforward calculation shows that for $W=0$, i.e., *no tunneling effects*, the four branches of magnetoplasmon modes with anticrossing are given approximately by

$$(\hbar\omega_{1+,2-})^2\approx\tfrac{1}{2}([(\hbar\omega_{20})^2+(\hbar\omega_{30})^2+A_{2,2}^{(2)}+A_{3,3}^{(1)}] \pm\{[(\hbar\omega_{20})^2-(\hbar\omega_{30})^2+A_{2,2}^{(2)}-A_{3,3}^{(1)}]^2+4A_{3,2}^{(1)}A_{2,3}^{(2)}\}^{1/2}) , \tag{11a}$$

$$(\hbar\omega_{1-})^2\approx(\hbar\omega_{10})^2+A_{1,1}^{(1)} , \tag{11b}$$

$$(\hbar\omega_{2+})^2\approx(\hbar\omega_{40})^2+A_{4,4}^{(0)} , \tag{11c}$$

where $A_{n,m}^{(j)}$ is q_z dependent and defined by

$$A_{n,m}^{(j)}(q_z)\equiv 4k_F\left[\frac{4e^2}{\epsilon_s}\right]\hbar\omega_{n0}F_{n,m}^{|j|}(q_z) . \tag{12}$$

Here, we only include the coupling of the resonant modes in Eq. (11a) and neglect all the other mode-mode couplings in Eqs. (11b) and (11c). Clearly the effect due to nonlocal interaction is evident from the depolarization shift displayed in Eqs. (11b) and (11c). Also, the anticrossing feature is described by Eq. (11a). Figure 1 is a plot of the magnetoplasmon excitation spectra as a function of magnetic field B for a quantum-dot superlattice. Here the electron energy bandwidth $W=0$ and the other parameters used in our calculation are $q_z=1.01\times10^{-4}$ Å^{-1}, $\epsilon_r=12.5$, $d=2\lambda_0=296$ Å, $m^*=0.067m_e$, $n_{3D}=5.2\times10^{16}$ cm^{-3}, and $\hbar\Omega_0=3.68$ meV. The single-particle excitation spectrum is split into branches. Anticrossing occurs at relatively low magnetic field, similar to the experimental results reported in Ref. 1. These are labeled ω_{2-} ($\Delta m=-2,\Delta n=0$) and ω_{1+} ($\Delta m=+1,\Delta n=0$). The highest branch is ω_{2+}:$\Delta m=0,\Delta n=1$ and the lowest branch is

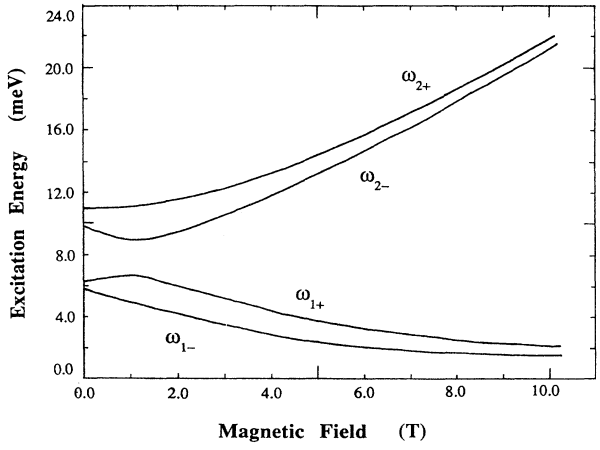

FIG. 1. B dependence of edge magnetoplasmon excitations for a quantum-dot superlattice. Here, the notations $\omega_{1\pm}$ correspond to the transitions $\Delta n=0,\Delta m=\pm1$, and $\omega_{2+}(\omega_{2-})$ to the transitions $\Delta n=1,\Delta m=0$ ($\Delta n=0,\Delta m=-2$).

ω_{1-}:$\Delta m=-1, \Delta n=0$. These modes ($|\Delta m|\neq 1$), which are forbidden for a parabolic confining potential, are allowed due to the level mixing and the deformation of the confining potential caused by nonlocal effects which were treated here in the self-consistent-field approximation. Both the resonant energy and the resonant position[1] are sensitive to the nonlocal effects (i.e. the single-particle confinement $\hbar\Omega_0$ and the electron number within each quantum dot). The degeneracies of $\omega_{1\pm}$ and $\omega_{2\pm}$ branches at zero magnetic field are lifted. At large magnetic fields, the normal branches (positive B dependence) develop into inter-Landau-level cyclotron modes, while the anomalous branches (negative B dependence) evolve into intra-Landau-level edge modes.

When there is electron tunneling between adjacent quantum dots, each branch is split into two. In order to compare quantitatively with the results in Ref. 2, we only give the splitting of the lowest branches $\omega_{1\pm}$ which are given approximately by

$$(\hbar\omega_{1-})^2 \approx (\hbar\omega_{10})^2 + \tfrac{1}{2}(A^{(1)}_{1,1}+B^{(1)}_{1,1}) \pm \tfrac{1}{2}[(A^{(1)}_{1,1}+B^{(1)}_{1,1})^2+8B^{(1)}_{1,1}(\hbar\omega_{10})^2]^{1/2}, \quad (13a)$$

$$(\hbar\omega_{1+})^2 \approx (\hbar\omega_{30})^2 + \tfrac{1}{2}(A^{(1)}_{3,3}+B^{(1)}_{3,3}) \pm \tfrac{1}{2}[(A^{(1)}_{3,3}+B^{(1)}_{3,3})^2+8B^{(1)}_{3,3}(\hbar\omega_{30})^2]^{1/2}, \quad (13b)$$

where

$$B^{(j)}_{n,m}(q_z) \equiv 4W\sin(k_F d)\left[\frac{4e^2}{\epsilon_s d}\right]\sin^2\left[\frac{q_z d}{2}\right]F^{(|j|)}_{n,m}(q_z) . \quad (14)$$

Here, we have neglected the coupling between the ω_{1+} mode and the ω_{1-} mode in deriving Eqs. (13a) and (13b). Figure 2 is a plot of the tunneling branches for ω_{1+} and ω_{1-}. To simulate weak tunneling, we take $W=0.5$ meV, $q_z=4.04\times10^5$ cm^{-1}, and all the other parameters are the same as in Fig. 1. These results suggest that the additional branches ($\omega_{t\pm}$ in our notation) found in the experiments of Lorke, Kotthaus, and Ploog[2] arise as a result of the strong coupling between quantum dots and the transfer of electrons between the dots. From Fig. 2, we know that the splitting is reduced at large magnetic field. This is due to the depletion of electrons in the lowest level, i.e., k_F is reduced as B increases from zero. Also, the degeneracy of the $\omega_{1\pm}$ modes at zero magnetic field is lifted. The upper branch will develop into inter-Landau-band cyclotron modes, while the lower branch will evolve into intra-Landau-band edge modes. For us to demonstrate this splitting analytically in Eqs. (13), we have used the weak-tunneling expansion for the irreducible polarizability. A more accurate treatment must involve next-nearest-neighbor hopping. In conclusion, the present calculations show that a single-particle model is not adequate for accounting for anticrossing. Our theory also explains quite nicely that the split branches in the experiments for a quantum-dot array are due to many-body effects and tunneling.

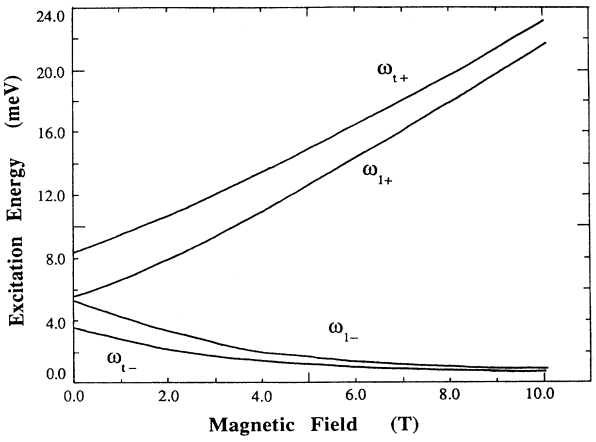

FIG. 2. B dependence of tunneling edge magnetoplasmon excitations for a quantum-dot superlattice. The notations $\omega_{1\pm}$ correspond to the transitions $\Delta n=0, \Delta m=\pm1$, and $\omega_{t\pm}$ to their split tunneling branches, respectively.

This work was partially supported by a grant from the Natural Sciences and Engineering Research Council of Canada. We gratefully acknowledge help from Chao Zhang for running our computer program.

[1]T. Demel, D. Heitmann, P. Grambow, and K. Ploog, Phys. Rev. Lett. **64**, 788 (1990).
[2]A. Lorke, J. P. Kotthaus, and K. Ploog, Phys. Rev. Lett. **64**, 2559 (1990).
[3]F. M. Peeters, Phys. Rev. B **42**, 1486 (1990).
[4]P. A. Maksym and T. Chakraborty, Phys. Rev. Lett. **65**, 108 (1990).
[5]P. Bakshi, D. Broido, and K. Kempa, Phys. Rev. B **42**, 7416 (1990).
[6]Danhong Huang and G. Gumbs (unpublished).
[7]Danhong Huang, Yun Zhu, Zhifang Lin, and Shixun Zhou, Phys. Rev. B **39**, 7713 (1989).